DEFORMED FRAGMENT OF METAL SHEET WT10-M305 – TIN BRONZE – IRON AGE – SWITZERLAND

Artefact name	Deformed fragment of metal sheet WT10-M305
Authors	Marianne. Senn (EMPA, Dübendorf, Zurich, Switzerland) & Christian. Degrigny (HE-Arc CR, Neuchâtel, Neuchâtel, Switzerland)
Url	/artefacts/444/

⌄ The object

Credit HE-Arc CR.

Fig. 1: Tin bronze sheet fragment (section and front side) (after Department of Prehistory, University of Zurich),

⌄ Description and visual observation

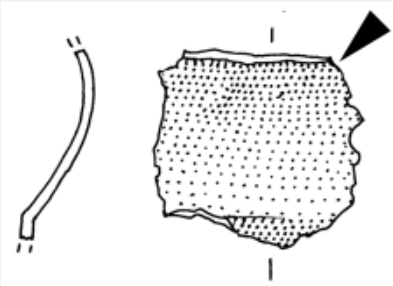|	
Description of the artefact	Sheet fragment with a dark green and grey powdery surface (patina) that might have been caused by exposure to high temperatures (Fig. 1). A green layer appears below the dark surface. Dimensions: L = 2.4cm; W = 2.3cm; WT = 4.8g.
Type of artefact	Metal sheet
Origin	Ritual place Wartau Ochsenberg, Sankt Gallen, Saint Gallen, Switzerland
Recovering date	Excavation in 1991
Chronology category	Iron Age
chronology tpq	500 B.C. ⌄
chronology taq	401 B.C. ⌄
Chronology comment	5th Century BC
Burial conditions / environment	Soil
Artefact location	Kantonsarchäologie, Sankt Gallen, Saint Gallen
Owner	Kantonsarchäologie, Sankt Gallen, Saint Gallen
Inv. number	WT10-M305
Recorded conservation data	Not conserved

Complementary information

Nothing to report.

Fig. 2: Location of sampling area,

Credit HE-Arc CR.

Stratigraphic representation: none.

Fig. 3: Micrograph of the cross-section showing the location of Figs. 5, 6, 8 and 9,

Credit HE-Arc CR.

Description of sample	The sample is a section from the top right corner of the sheet (Fig. 2). Its dimensions are: L = 2.5mm and W = 2.3mm. The metal is surrounded on three sides by corrosion products. Intergranular corrosion has developed throughout the metal section (Fig. 3).
Alloy	Tin Bronze
Technology	Secondary recrystallization (produced by burning) after cold working
Lab number of sample	MAH 92-5-2-003
Sample location	Musées d'art et d'histoire, Genève, Geneva

Responsible institution	Musées d'art et d'histoire, Genève, Geneva
Date and aim of sampling	1992, examination of the corrosion layer

Complementary information

Nothing to report.

⌄ Analyses and results

Analyses performed:
Metallography (etched with ferric chloride reagent), Vickers hardness testing, ICP-OES, SEM/EDS, Raman spectroscopy.

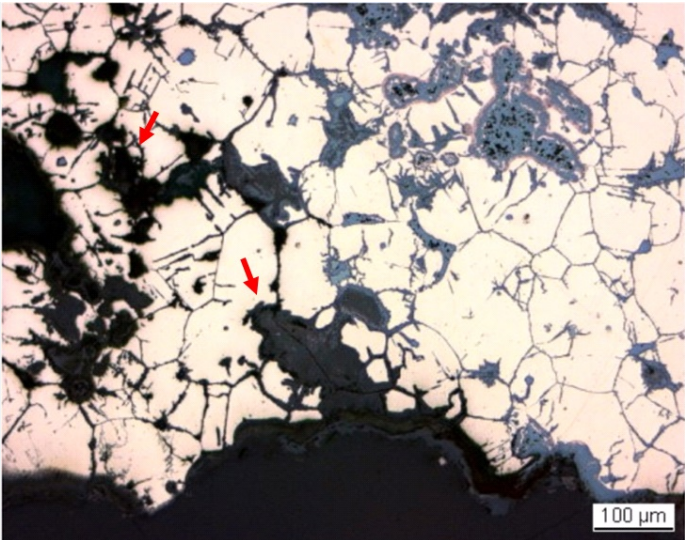## ⌄ Non invasive analysis

⌄ Metal

The remaining metal is a porous (red arrows on Fig. 5) tin bronze (Table 1). Five analyses were carried out. S was detected in the non-corroded part of the metal (2 measurements) while P was present only in the corroded metal (3 measurements). As no major difference in the composition was observed (comparison of relative standard deviation, RSD) all analyses were used to calculate the median value. Inter- and transgranular corrosion has developed so extensively that all grain boundaries and twin lines are outlined (Fig. 5). After etching, the metal shows annealed polygonal grains with a few twins and slip lines below the surface (Fig. 6). The slip lines are restricted to the right side of the sample where the metal is best preserved (Fig. 6). The grain size varies between 50 and 170μm, due to an excessively long or hot annealing procedure leading to a grain coarsening. Small copper sulphide inclusions appear in blue (Fig. 6). The average hardness of the metal is HV1 90.
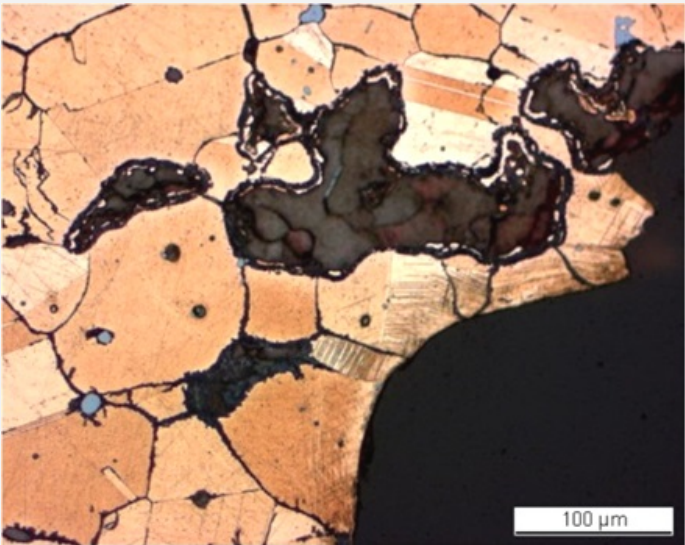
Elements	Cu	Sn	As	S*	P**	Co	Ni	Pb	Sb	Ag	Zn	Fe	Bi
mass% (median value of 5 measurements)	83.13	16	0.26	0.1	0.07	0.032	0.025	0.02	0.02	0.009	0.002	<	0.002
RSD %	2	9	13	25	45	3	5	41	15	12	6	<	43

Table 1: Chemical composition of the metal. Analytical method: LA-ICP-MS, Laboratory of Basic Aspects of Analytical Chemistry at the Faculty of Chemistry, University of Warsaw, PL. *S is only present in the metal, whereas **P indicates the presence of corrosion products in the analysed metal.

Fig. 5: Micrograph of the metal sample from Fig. 3 (detail), unetched, bright field. Extensive inter- and transgranular corrosion has developed within the metal. Possible large pores are visible (arrows) inside the remaining metal,

Credit HE-Arc CR

Fig. 6: Micrograph of the metal sample from Fig. 3 (detail), etched, bright field. We observe pink-orange polygonal grains with twins and slip lines as well as copper sulphide inclusions (in blue),

Credit HE-Arc CR.

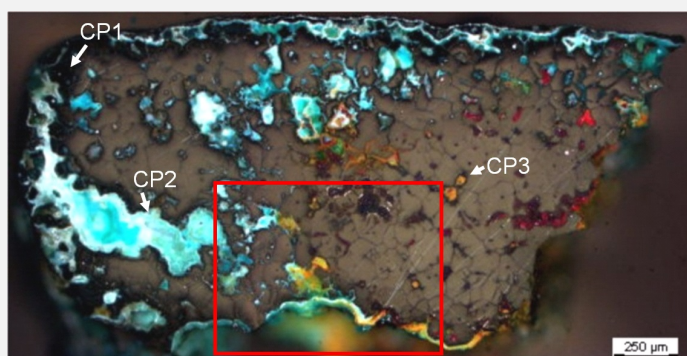|	
Microstructure	Large polygonal grains with few twins + strain lines
First metal element	Cu
Other metal elements	As, Sn

Complementary information

Nothing to report.

⩔ Corrosion layers

The corrosion crust varies in thickness between 60 and 150µm (Fig. 3). In bright field, it appears dark-grey (Fig. 5) and consists of two layers (CP1 and CP2). The inner layer is dark-grey and dense while the thin outer layer is slightly lighter coloured. Within the metal, the corrosion products are light-grey (CP3, Fig. 5). Under polarized light, the corrosion layer turns blue-green with dark-blue areas (Figs. 7 and 8) whereas corrosion products inside the metal are either light-blue or red-orange (Figs. 7 and 8). The red corrosion products (CP3) have the composition of cuprite/Cu_2O while the orange compounds (also CP3) are enriched in Sn (Table 2). The blue-green corrosion products (CP2) both within the remaining metal and on the surface are even richer in Sn and O, and contain some P (Table 2 and Fig. 9). The thin, irregular dark-grey surface layer (CP1) is enriched in P, Fe, Si and Al (Table 2 and Fig. 9). XRD analyses of powdery particles sampled from the thin, dark surface corrosion layer (CP1) indicate the presence of tenorite/CuO and cassiterite/SnO_2 (Museum report 1992). The Raman spectra of this layer (Fig. 10) confirmed the presence of tenorite.
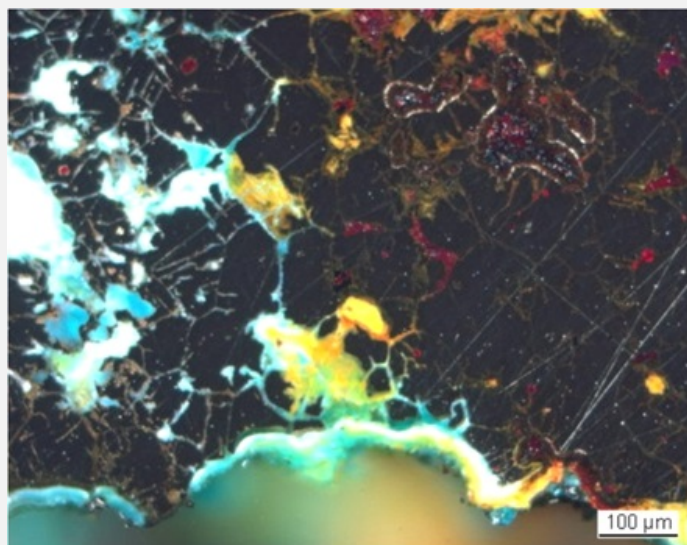
Elements	O	Cu	Sn	Si	Fe	P	As	Total
CP1, outer dark-grey corrosion layer. Fig 7	34	16	49	<	3.4	3.0	0.86	108
CP2, blue-green middle corrosion layer. Fig. 7	40	21	41	1.4	<	1.7	0.58	106
CP3, Red corrosion product (average of 2 similar analyses). Fig. 7	11	95	<	<	<	<	<	106
CP3, Orange corrosion product (average of 2 similar analyses). Fig. 7	24	54	30	0.6	<	<	0.59	109
Blue-green corrosion product. Fig. 8	32	21	51	1.1	<	<	1.0	106
Blue-green inner corrosion layer. Fig. 8	34	22	39	0.8	<	1.4	<	98

Table 2: Chemical composition (mass %) of the different corrosion products and layers from Figs. 7 and 8. Method of analysis: SEM/EDS, Laboratory of Analytical Chemistry, Empa.
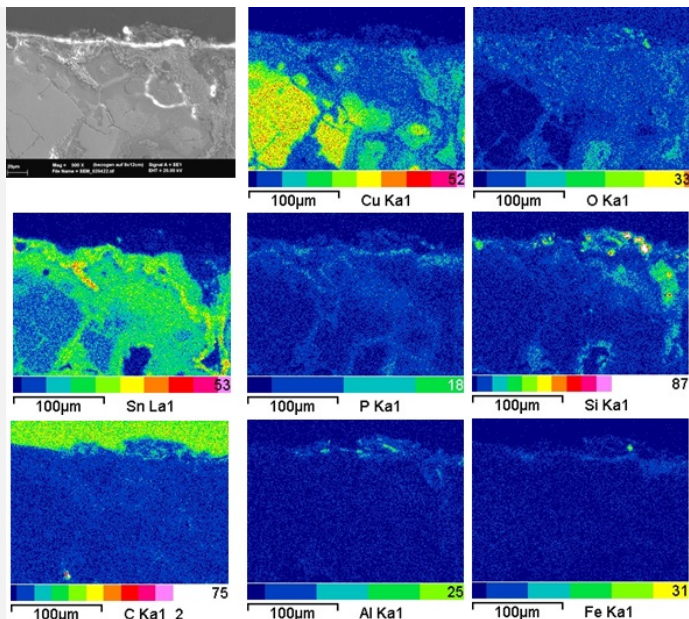

Credit HE-Arc CR.

Fig. 7: Micrograph of the cross-section (same as Fig. 3) and corresponding to the stratigraphy of Fig. 4, polarised light, showing the location of Fig. 8,
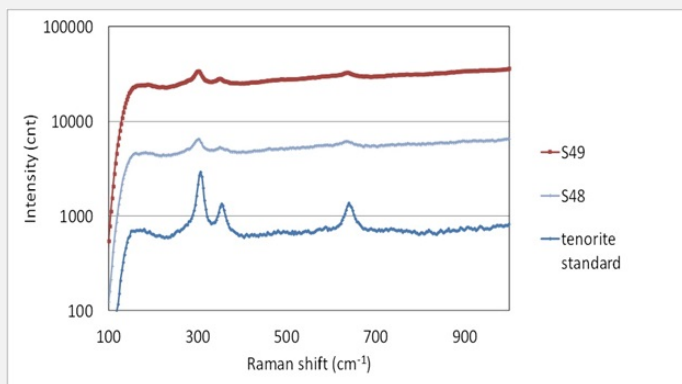

Credit HE-Arc CR.

Fig. 8: Micrograph (same as Fig. 5), polarised light. In black the metal. Blue-green, orange and red corrosion products are found in the porous metal and along the grain boundaries,
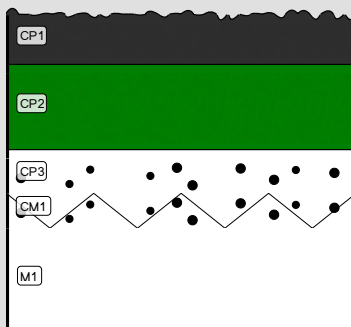
Fig. 9: SEM image, SE-mode, and elemental chemical distribution of the selected area from Fig. 3. Method of examination: SEM/EDS, Laboratory of Analytical Chemistry, Empa,

Credit Empa.

Fig. 10: Raman spectra of the outer dark corrosion layer (S48 and S49) compared to a tenorite standard spectrum. Settings: laser wavelength 532nm, acquisition time 20s for S48 and 100s for S49, one accumulation, filter D1 (7.5-8mW), hole 500, slit 80, grating 600. Method of analysis: Raman spectroscopy, Lab of Swiss National Museum, Affoltern a. Albis ZH,

Credit SNM.

Corrosion form	Uniform - intergranular
Corrosion type	Mostly type II with locally type I (Robbiola)

Complementary information

Nothing to report.

⌄ MiCorr stratigraphy(ies) – CS

Fig. 4: Stratigraphic representation of the object in cross-section using the MiCorr application. The characteristics of the strata are only accessible by clicking on the drawing that redirects you to the search tool by stratigraphy representation. This representation can be compared to Fig. 7, Credit HE-Arc CR.

⌄ Synthesis of the binocular / cross-section examination of the corrosion structure

Corrected stratigraphic representation: none.

⅋ Conclusion

The tin bronze sheet shows traces of cold working but has been exposed to an extended or excessively hot annealing process. According to Northover (Northover in preparation), the relative lack of twins and their large size confirm a prolonged annealing process. Furthermore large grains, large twins and extensive intergranular corrosion are characteristic of objects that have been exposed to a hot reducing flame either in a house fire or on a funeral pyre. All corrosion products except the cuprite are Sn enriched. The enrichment in P of the surface layer might be due to an environment rich in organic material (for example bones). Tenorite analysed by XRD and Raman spectroscopy is very rare in ancient Cu corrosion and must be interpreted as a further tracer for Cu corrosion in burning context. The original surface of the metal has been destroyed resulting in a type 2 corrosion layer after Robbiola et al. 1998. Only locally in the areas where tenorite is preserved does type 1 patina occur.

⅋ References

References on object and sample
Reference object
1. Publication in preparation (Biljana Schmid-Sikimic).
Reference sample
2. Degli Agosti, M., Santoro, I., Senn, M., Untersuchungen zur Brandpatina an Kupferlegierungen. In: Schmid-Sikimic, B. in preparation.
3. Northover, P., Untersuchungen an Fragmenten einiger Negauer-Helme. In Schmid-Sikimic, B. in preparation.
4. Rapport d'examen, Laboratoire Musées d'art et d'histoire, Genève 92-5-2 (1992).
References on analytic methods and interpretation
5. Robbiola, L., Blengino, J-M., Fiaud, C. (1998) Morphology and mechanisms of formation of natural patinas on archaeological Cu-Sn alloys, Corrosion Science, 40, 12, 2083-2111.